Arch. Metall. Mater. **68** (2023), 3, 1087-1102

DOI: https://doi.org/10.24425/amm.2023.145479

A. JAKHAR[1], L. SHARMA[2*], P. RATH[1], S. KUMAR MAHAPATRA[1]

SIMILARITY SOLUTION FOR PHASE CHANGE OF DILUTE BINARY ISOMORPHOUS ALLOY WITH DENSITY VARIATION DURING PHASE CHANGE

A similarity solution for conduction dominated solidification of a dilute binary isomorphous alloy has been developed. The effect solidification due to density change during phase transformation has been highlighted and investigated in detail. The governing equations for solid, liquid and mushy phase has been proposed, taking into account the effect of shrinkage or expansion due to density change during phase change. The thermo-physical properties (thermal conductivity and specific heat), equilibrium temperature and phase fraction are evaluated within the mushy zone using averaging technique. The effect of equilibrium and non-equilibrium solidification is investigated using Lever and Scheil's rule models respectively. In addition, the effect of boundary and initial temperature on solidification behavior of the alloy is also addressed. It has been observed that the interface (liquidus and solidus) moves faster with increase in density ratio and decrease in boundary and initial temperature. No major changes in temperature distribution and interface position has been observed with variation partition coefficient and microscale behavior model (Lever rule and Scheil's rule).

Keywords: Binary alloy; Variable density; similarity variable; Conduction dominated; Mushy zone

1. Introduction

Generally, most of the investigations on derivation of analytical expressions on phase change has been limited to single component systems. Özişik [1] provided list of exacts solution in the book for single component phase change in a semi-infinite domain for different kind of boundary conditions assuming interface to be sharp. Subsequently, Alexiades and Solomon [2] presented extensive list of cases in the book that examined the effect of thermo-physical properties (specific heat, latent heat, thermal conductivity and density) on phase change behavior of single component systems in one dimensional domain. This is carried out by analyzing the front position and movement during solidification and melting. Turkyilmazoglu [3] proposed material movement for Stefan problems with moving boundary problem. Ceretani and Tarzia [4] developed exact solution for one-dimensional two-phase Stefan problem for a convective boundary condition. Barannyk et al. [5] proposed exact solution with heat generation and having heat flux boundary condition. Parhizi and Jain [6] used perturbation method to obtain solution for one dimensional Stefan problem with time dependent heat flux.

Experimental investigations have been carried out for the phase change of binary alloy [7,8]. Different type of numerical methods like finite element method, finite volume method, boundary element method etc. [9-13] have been proposed which assist in understanding the physics of the phase change process of the binary alloy. The analytical models are very much useful for analysis as the results are reliable as compared to that obtained from numerical models on phase change which are error prone. However, one of the major drawbacks associated with analytical models is that it is quite challenging to formulate and derive exact solution for complex geometry. The derived analytical expression can be used for verification of physics of new numerical schemes for phase change process.

The physics and behavior of binary alloy phase change is different from that of single component phase change. In case of single component alloy the phase change takes place at a fixed temperature, whereas for a binary alloy it takes over a temperature range. This leads to formation of two phase zone which is mixture of both solid phase and liquid phase called mushy zone. The phase change associated transformation and solute segregation takes place within the mushy zone which makes it vital to investigate conjugate heat transfer physics in this zone. A limited

[1] SCHOOL OF MECHANICAL SCIENCES, IIT BHUBANESWAR, BHUBANESWAR, 751012, INDIA
[2] CHANDIGARH UNIVERSITY, UNIVERSITY CENTRE OF RESEARCH & DEVELOPMENT, MOHALI-140413, PUNJAB

* Corresponding author: lochan.e9455@cumail.in

number of analytical studies exists in literature that have derived exacts solution for binary alloy phase change [14-17]. Chung et al. [14] proposed an analytical solution for conduction dominated solidification of binary mixtures by assuming different thermal conductivities for solid and liquid. Chakraborty and Dutta [15] developed an analytical solution for unidirectional solidification of the binary eutectic mixture using both Lever rule model and Scheil's rule model. The governing equations within the mushy zone were modelled using averaging technique. Voller [16] derived similarity solution for an under cooled binary alloy. Assunção et al. [18] Planella et al. [19-21] proposed small time semi analytical solution for solidification of binary alloy. Chaurasiya et al. [22] developed analytical solution for solidification of binary alloy with imposed boundary movement.

The present work addresses the effect of shrinkage and expansion due to density variation during phase change of dilute binary isomorphous alloy. In most practical cases the density is assumed to be constant. During the phase change, there is significant density change of approximately –20 to 20% depending on the material [23]. In most cases, like that of alloy and other non-metallic elements and compounds, shrinkage occurs during solidification, whereas in the case of water and polymers expansion observed during solidification. In our previous work, an analytical solution was although developed for solidification of binary alloy taking into effect of phase density but it is valid for phase transformation with sharp interface [17]. However, generally solid and liquid phases are separated by a mushy zone (having significant width) which has varying fusion temperature (depending on concentration and morphology). All phase transformation occurs within the mushy zone. Hence, the focus of the present model concentrated on developing an analytical solution using similarity variable by considering density variation during phase change and highlighting the transport mechanism in the mushy zone developed during the solidification of a binary isomorphous alloy. A semi-analytical solution has been proposed for both equilibrium and non-equilibrium solidification with the help of Lever and Scheil's rule model. The developed analytical model could be used for validation of the numerical results obtained by simulation of binary alloy phase change process such as casting and selective laser melting.

2. Problem description

The thermophysical properties of Cu-Ni binary isomorphous alloy composition which is dilute in copper is chosen for analysis in present study which can also be carried on binary eutectic alloy system. The physical schematic of the present problem is shown in Fig. 1. Initially, the superheated melt of a binary alloy is at a temperature $T_{initial}$, which is above the equilibrium melting temperature of the alloy. Suddenly, the left wall ($x = 0$) temperature was dropped to T_b, which is below the equilibrium melting point of the alloy. As a result, solidification starts from the left cold isothermal wall and proceeds in a direction perpendicular to the wall.

Following assumptions have been taken while developing the binary mixture model.

1. The thermo-physical properties like thermal conductivity and specific heat are assumed to be invariant with temperature, position and time. Within the mushy zone, these properties are obtained by interpolating it as a function of the average liquid fraction.
2. The density is assumed to be constant in solid, liquid and mushy phase though it may be different in each zone.
3. The solidus and liquidus interface is assumed to be sharp and straight for the entire period of solidification.
4. The temperature is assumed to vary only unidirectionally along the direction of solidification.
5. Conduction is assumed to be a dominating mode of heat transfer, while convective and radiative effects are neglected.
6. Natural convection due to buoyancy effects is neglected.
7. Species diffusion is assumed to be negligible as compared to thermal diffusion in solid phase.
8. The model assumes uniform composition of the binary alloy all throughout the solidification process.
9. The partition coefficient value is assumed to be fixed and invariant with change in time, composition or temperature.
10. Coupling between temperature and concentration is governed by the phase diagram for the respective mixture, while between concentration and phase fraction is obtained from the Lever rule model, Scheil's rule model or Broody Flemming's model depending on the diffusion rate of solute in solid and mushy phase.

The properties for pure Copper, pure Nicker and Copper Nickel alloy (0.05%, 0.1% and 0.15%) used in computing certain primitive variables as well as the derived parameters are as given in TABLE 1.

3. Governing equations

Incorporating the assumptions considered in the proposed model, a set of governing equations are obtained for solid, liquid and mushy zone, which is given by Eqs. (1)-(3) [15,17].

$$\frac{1}{\alpha_S}\frac{\partial T_S}{\partial t}=\frac{\partial^2 T_S}{\partial x^2},\ 0<x<x_S \text{ (Solid phase)} \tag{1}$$

$$\frac{1}{\alpha_M}\frac{\partial T_M}{\partial t}+\frac{(1-f_S)}{\alpha_M}\left(\frac{\rho_S}{\rho_L}-1\right)\frac{dx_S}{dt}\frac{\partial T_M}{\partial x}= =\frac{\partial^2 T_M}{\partial x^2}+\frac{\rho_M L_f}{k_M}\frac{\partial f_S}{\partial t},\quad x_S<x<x_L \text{ (Mushy zone phase)} \tag{2}$$

$$\frac{1}{\alpha_L}\frac{\partial T_L}{\partial t}+\frac{1}{\alpha_L}\left(\frac{\rho_S}{\rho_L}-1\right)\frac{dx_S}{dt}\frac{\partial T_L}{\partial x}=\frac{\partial^2 T_L}{\partial x^2},\quad x_L<x<\infty \text{ (Liquid phase)} \tag{3}$$

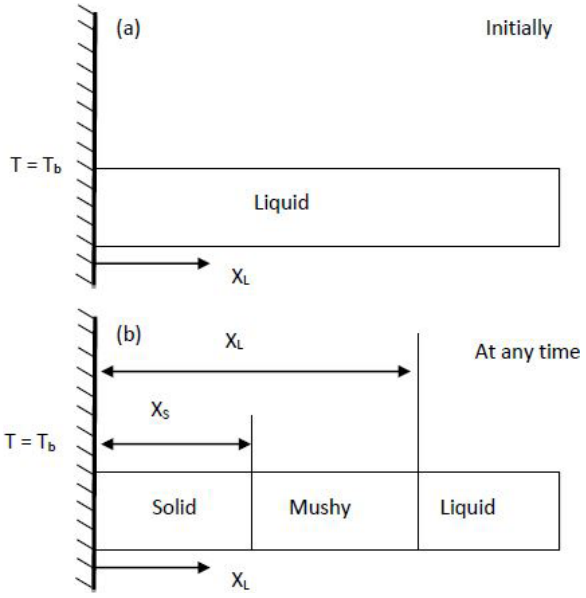

Fig. 1. The problem domain with respective phases at (a) initial time (b) at a given time during solidification

Eqs. (1), (2) and (3) represents the energy equations governing three phases that are solid, liquid and mushy zone. There is an extra term that comes on left-hand side of the energy equation governing liquid and mushy zone phase, to take care of heat transfer due to density change. In addition, there is a second term on right-hand side of equation governing mushy zone phase. This term account for the latent heat generated within the mushy zone during solidification of the binary alloy. Using the chain rule for transient part of this term we get,

$$\frac{\partial f_S}{\partial t} = \frac{\partial f_S}{\partial T_M}\frac{\partial T_M}{\partial t} \tag{4}$$

Substituting Eq. (4) in Eq. (2) and rearranging we get following equation for mushy phase

$$\left(\frac{1}{\alpha_M} - \frac{\rho_M L_f}{k_M}\frac{\partial f_S}{\partial T_M}\right)\frac{\partial T_M}{\partial t} + \\ + \frac{(1-f_S)}{\alpha_M}\left(\frac{\rho_S}{\rho_L} - 1\right)\frac{dx_S}{dt}\frac{\partial T_M}{\partial x} = \frac{\partial^2 T_M}{\partial x^2},\ x_S < x < x_L \tag{5}$$

3.1. Initial, interface and boundary conditions

Initially, the whole liquid is maintained at a uniform temperature and concentration, which is represented mathematically by Eq. (6).

$$T = T_{initial}\ 0 < x < \infty \text{ at } t = 0 \tag{6}$$

The boundary conditions at left cold wall and on the other side of the semi-infinite domain can be given as

$$T = T_b \text{ at } x = 0 \tag{7}$$

$$T_{initial} = T_b \text{ as } x \to \infty \tag{8}$$

Boundary conditions at the solidus and liquids interfaces can be given as

$$T_M = T_{solidus} \text{ at } x = x_S \tag{9}$$

$$k_S\left(\frac{\partial T_S}{\partial x}\right)\Big|_{x=x_S^-} - k_M\left(\frac{\partial T_M}{\partial x}\right)\Big|_{x=x_S^+} = \\ = \left(1 - f_{S,solidus}\right)\rho_S L_f \frac{dx_S}{dt} \text{ at } x = x_S \tag{10}$$

$$T_M = T_{liquidus} \text{ at } x = x_L \tag{11}$$

$$k_M\left(\frac{\partial T_M}{\partial x}\right)\Big|_{x=x_L^-} - k_L\left(\frac{\partial T_L}{\partial x}\right)\Big|_{x=x_L^+} = \\ = f_{S,liquidus}\rho_L L_f \frac{dx_L}{dt} \text{ at } x = x_L \tag{12}$$

3.2. Non-dimensionalization

For systematic parametric analysis, the governing equations along with the boundary conditions and interface conditions are non-dimensionalized using the dimensionless parameters as defined below.

$$\theta_S = \frac{T_S - T_b}{T_{solidus} - T_b},\ \theta_M = \frac{T_M - T_{solidus}}{T_{melt} - T_{solidus}} \\ \text{and } \theta_L = \frac{T_L - T_{initial}}{T_{liquidus} - T_{initial}} \tag{13}$$

$$\theta_E = \frac{T_{solidus} - T_b}{T_{melt} - T_{solidus}},\ r_{MS} = \frac{k_M}{k_S} \\ \text{and } St = \frac{Cp\left(T_{melt} - T_{solidus}\right)}{L_f} \tag{14}$$

$$\theta_{M,liquidus} = \frac{T_{liquidus} - T_{solidus}}{T_{melt} - T_{solidus}},\ r_{LS} = \frac{k_L}{k_S} \\ \text{and } \theta_{initial} = \frac{T_{liquidus} - T_{initial}}{T_{melt} - T_{solidus}} \tag{15}$$

On substituting the above dimensionless parameters in Eqs. (1), (3) and (5), will result in following non-dimensional form of governing equations.

$$\frac{1}{\alpha_S}\frac{\partial \theta_S}{\partial t} = \frac{\partial^2 \theta_S}{\partial x^2},\ 0 < x < x_S \text{ (Solid phase)} \tag{16}$$

$$\left(\frac{1}{\alpha_M} - \frac{\rho_M L_f}{k_M}\frac{\partial f_M}{\partial T_M}\right)\frac{\partial \theta_M}{\partial t} + \\ + \frac{(1-f_S)}{\alpha_M}\left(\frac{\rho_S}{\rho_L} - 1\right)\frac{dx_S}{dt}\frac{\partial \theta_M}{\partial x} = \frac{\partial^2 \theta_M}{\partial x^2}, \\ x_S < x < x_L \text{ (Mushy phase)} \tag{17}$$

$$\frac{1}{\alpha_L}\frac{\partial\theta_L}{\partial t}+\frac{1}{\alpha_L}\left(\frac{\rho_S}{\rho_L}-1\right)\frac{dx_S}{dt}\frac{\partial\theta_L}{\partial x}=$$
$$=\frac{\partial^2\theta_L}{\partial x^2},\ x_L<x<\infty \text{ (Liquid phase)} \tag{18}$$

Using the dimensionless parameters defined in Eqs. (13)-(15), the boundary and interface conditions can be represented in non-dimensional form as.

$$\theta_S=0 \text{ at } x=0 \tag{19}$$

$$\theta_L=0 \text{ at } x\to 0 \tag{20}$$

Similarly, on substituting non-dimensional parameters in interface conditions given by Eqs. (9)-(12) results in

$$\theta_S=1,\ \theta_{M,solidus}=1, \text{ at} \tag{21}$$

$$\theta_E\left.\frac{\partial\theta_S}{\partial x}\right|_{x=x_S^-}-r_{MS}\left.\frac{\partial\theta_M}{\partial x}\right|_{x=x_S^+}=\frac{2x_S\left(1-f_{S,solidus}\right)}{St} \tag{22}$$

$$\theta_L=1 \text{ at } x=x_L \tag{23}$$

$$r_{MS}\theta_{M,liquidus}\left.\frac{\partial\theta_M}{\partial x}\right|_{x=x_L^-}-r_{LS}\,\theta_{initial}\left.\frac{\partial\theta_L}{\partial x}\right|_{x=x_L^+}=$$
$$=\frac{\rho_L}{\rho_S}\frac{2x_L f_{S,liquidus}}{St} \tag{24}$$

3.3. Similarity transformation

A similarity transformation is applied through similarity parameter $\eta=xg(t)$ where, $g(t)=\frac{1}{2\sqrt{\alpha_S t}}$, to the Eqs. (16)-(18) and are transformed into ordinary differential equations as given below.

Solid phase

$$\frac{d^2\theta_S}{d\eta^2}+2\eta\frac{d\theta_S}{d\eta}=0, \text{ for } 0<\eta<\eta_S \tag{25}$$

Mushy zone phase

$$\frac{d^2\theta_M}{d\eta^2}+\left(2a_M\eta+b_M\right)\frac{d\theta_M}{d\eta}=0, \text{ for } \eta_S<\eta<\eta_L \tag{26}$$

Where

$$a_M=\frac{\alpha_S}{\alpha_M'},\ b_M=-2\left(1-f_S\right)\eta_S\frac{\alpha_S}{\alpha_M}\left(\frac{\rho_S}{\rho_L}-1\right)$$
$$\text{and } \frac{1}{\alpha_M'}=\frac{1}{\alpha_M}-\frac{\rho_M L_f}{k_M}\frac{\partial f_S}{\partial T_M}$$

Liquid phase

$$\frac{d^2\theta_L}{d\eta^2}+\left(2a_L\eta+b_L\right)\frac{d\theta_L}{d\eta}=0, \text{ for } \eta_L<\eta<\infty \tag{27}$$

Where

$$a_L=\frac{\alpha_S}{\alpha_L} \text{ and } b_L=-2\eta_S\frac{\alpha_S}{\alpha_L}\left(\frac{\rho_S}{\rho_L}-1\right)$$

3.4. Solution to the governing equations

The exact solution for the solid and liquid phase can be directly obtained and is given as

$$T_S=T_b+\left(T_{solidus}-T_b\right)\frac{erf\left(\eta\right)}{erf\left(\eta_S\right)},\ 0<\eta<\eta_S \tag{28}$$

$$T_L=T_{initial}+\left(T_{liquidus}-T_{initial}\right)\frac{erfc\left(\sqrt{a_L}\eta+\frac{b_L}{2\sqrt{a_L}}\right)}{erfc\left(\sqrt{a_L}\eta+\frac{b_L}{2\sqrt{a_L}}\right)},$$
$$\eta_L<\eta<\infty \tag{29}$$

In the present analysis, the study is majorly focused on mushy zone. In case of binary alloy, all phase transformation occurs within the mushy zone. Most of the work on analytical solution that has been obtained is for binary isomorphous alloy, in which liquid fraction within the mushy zone varies linearly with temperature. In the current context the relation between temperature and liquid fraction is obtained indirectly. Based on the linearization of the liquidus and solidus slope as an assumption as in Fig. 2, we get relation between temperature and concentration in a manner, as given in Eqs. (30) and (31).

From the eutectic phase diagram (Fig. 2) we will get the following equations

$$\frac{T_M-T_{melt}}{T_{solidus}-T_{melt}}=\frac{C_S}{C_i} \tag{30}$$

$$\frac{T_M-T_{melt}}{T_{liquidus}-T_{melt}}=\frac{C_L}{C_i} \tag{31}$$

The relation between temperature and liquid fraction can be obtained by obtaining an expression which relates concentration and liquid fraction. With the help of Lever rule model (for equilibrium solidification) and Scheil's rule model (for non-equilibrium solidification) a relation between concentration and liquid fraction, can be expressed as

$$\frac{C_S}{C_i}=\frac{1}{f_S+\left(1-f_S\right)/k_p} \text{ (Lever rule model)} \tag{32}$$

$$\frac{C_L}{C_i}=\left(1-f_S\right)^{\left(k_p-1\right)} \text{ (Scheil's rule model)} \tag{33}$$

Using Eqs. (30)-(33) a relation between temperature and liquid fraction can be obtained, which on further simplification results in rate of liquid fraction variation with temperature as given in Eqs. (34)-(35), for equilibrium and non-equilibrium solidification.

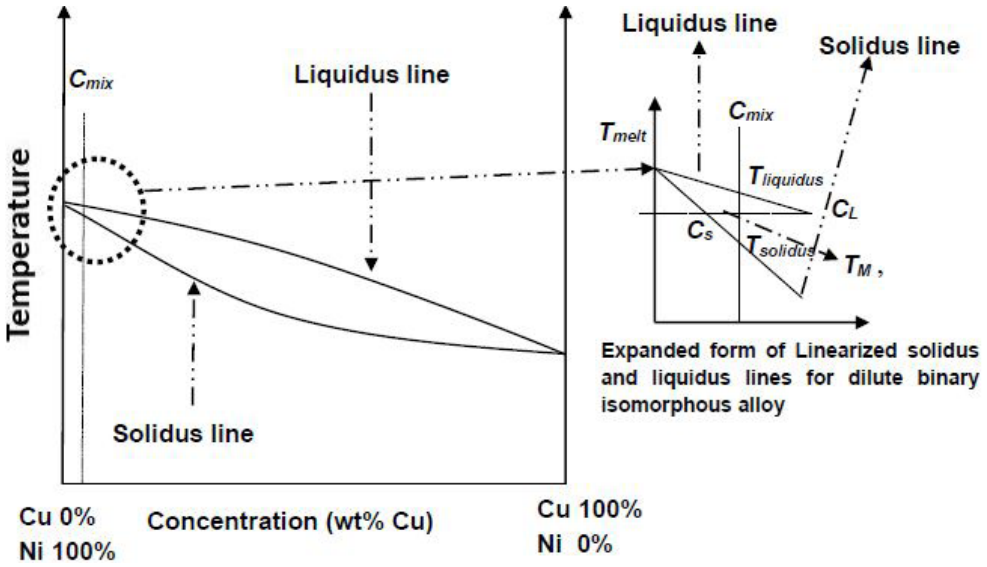

Fig. 2. Phase diagram for binary isomorphous alloy

Lever rule model (Equilibrium solidification)

$$\frac{\partial f_S}{\partial T_M} = \frac{1}{1-1/k_p}\frac{\left(T_{melt}-T_{solidus}\right)}{\left(T_M-T_{melt}\right)^2} \tag{34}$$

Scheil's rule model (Non-equilibrium solidification)

$$\frac{\partial f_S}{\partial T_M} = \frac{1}{\left(1-k_p\right)}\left(\frac{1}{T_{liquidus}-T_{melt}}\right)^{\left(\frac{1}{k_p-1}\right)}\left(T_M-T_{melt}\right)^{\frac{\left(2-k_p\right)}{\left(k_p-1\right)}} \tag{35}$$

To find the term $\partial f_S/\partial T_M$ in Eq. (17), Eq. (34) and Eq. (35) can be used. The overall average change of solid fraction with respect to change in temperature in the mushy zone could be expressed as

$$\left\langle \frac{\partial f_S}{\partial T_M} \right\rangle_{avg} = \left(\int_{T_{solidus}}^{T_{liquidus}} \frac{\partial f_S}{\partial T_M} dT_M / \Delta T \right)$$
$$\text{where } \Delta T = T_{liquidus} - T_{solidus} \tag{36}$$

Eq. (36) represents an averaged solid fraction over an interval between liquidus and solidus temperatures. There is no explicit analytical expression that could relate variation of solid fraction with temperature within the mushy zone. One advantage of using averaging is that the term $\partial f_S/\partial T_M$ can be easily found out over mushy range, making approach to our current problem quite simpler and straightforward.

Using Eq. (34) and Eq. (36) and integration over mushy zone range gives the average value of $\partial f_S/\partial T_M$ represented by $\left\langle f_S^T \right\rangle_{avg}$ for equilibrium solidification as

$$\left\langle f_S^T \right\rangle_{avg} = \frac{1}{\left(1-1/k_p\right)\left(T_{melt}-T_{liquidus}\right)} \tag{37}$$

Using the value of $\left\langle f_S^T \right\rangle_{avg}$ obtained from Eq. (37), the average equilibrium temperature over a mushy range can be obtained with the help of Eq. (34) as

$$T_{eq} = T_{melt} - \sqrt{\begin{matrix} T_{melt}^2 - T_{melt}T_{liquidus} - T_{melt}T_{solidus} + \\ + T_{solidus}T_{liquidus} \end{matrix}} \tag{38}$$

The equilibrium average solid fraction can be obtained from Eq. (30) and Eq. (32) as

$$f_{s,eq} = \frac{1}{\left(1-1/k_p\right)}\left(\frac{T_{melt}-T_{solidus}}{T_{melt}-T_{eq}} - \frac{1}{k_p}\right) \tag{39}$$

Similarly, combining Eqs. (35)-(36) and integrating over the given mushy range, the expression for average value of $\partial f_S/\partial T_M$ using Scheil's rule Model can be obtained as

$$\left\langle f_S^T \right\rangle_{avg} = \frac{1}{\left(T_{liquidus}-T_{solidus}\right)}\left(\left(\frac{T_{melt}-T_{solidus}}{T_{melt}-T_{liquidus}}\right)^{-\frac{1}{1-k_p}} - 1\right) \tag{40}$$

With the help of $\left\langle f_S^T \right\rangle_{avg}$ obtained from Eq. 40, the average equilibrium temperature over a mushy range can be obtained using Eq. (35) and Eq. (40) as

$$T_{eq} = T_{melt} - \left[\left(1-k_p\right)B\right]^{\frac{1-k_p}{2-k_p}} \tag{41}$$

Where

$$B = \frac{1}{T_{liquidus}-T_{solidus}}\left[\begin{matrix} \left(T_{melt}-T_{liquidus}\right)^{-\frac{1}{1-k_p}} - \\ \left(T_{melt}-T_{solidus}\right)^{-\frac{1}{1-k_p}} \end{matrix}\right]$$

The average equilibrium solid fraction can be obtained from Eq. (31) and Eq. (33) as

$$f_{S,eq} = 1 - \left(\frac{T_{melt} - T_{eq}}{T_{melt} - T_{liquidus}} \right)^{-\frac{1}{1-k_p}} \tag{42}$$

On obtaining $f_{S,eq}$, the average thermo-physical properties within the mushy zone can be obtained as

$$\varphi_{M,eq} = f_{S,eq}\varphi_S + \left(1 - f_{S,eq}\right)\varphi_L \tag{43}$$

Where φ may be density, thermal conductivity, specific heat etc.

Once all the values required for solving Eq. (26) are obtained, we could obtain a semi-analytical expression for the mushy zone. A step-by-step procedure for finding out the position of mushy zone is summarized below.

1. Express temperature of mushy zone as a function of concentration, from the eutectic phase diagram related by expression $T_M = F(C_L)$ as given by Eqs. (30) and (31).
2. Find out the concentration as a function of solid fraction, given by relation $C_L = F(f_S)$ as given in Eqs. (32) and (33) for Lever and Scheil's rule models respectively.
3. Using Steps 1 and 2, relation between temperature and solid fraction can be obtained as $T_M = F(f_S)$.This relation could be obtained from different models, mainly Lever rule model and Scheil's rule model.
4. Calculate $\partial f_S/\partial T_M$ as given in Eqs. (34)-(35).
5. Calculate the average value of $\partial f_S/\partial T_M$ from Eq. (36).
6. Obtain $f_{S,eq}$, T_{eq} and $\varphi_{M,eq}$.
7. Substitute all the required input average properties to solve Eq. (26) for θ_M in the mushy zone.

On following systematic execution from Step-1 to Step-7, the temperature distribution within the mushy zone can be obtained as

$$T_M = T_{solidus} + \left(T_{liquidus} - T_{solidus}\right) \times \beta,\ \eta_S < \eta < \eta_L \tag{44}$$

Where

$$\beta = \frac{erf\left(\sqrt{a_M}\eta + \frac{b_M}{2\sqrt{a_M}}\right) - erf\left(\sqrt{a_M}\eta_S + \frac{b_M}{2\sqrt{a_M}}\right)}{erf\left(\sqrt{a_M}\eta_L + \frac{b_M}{2\sqrt{a_M}}\right) - erf\left(\sqrt{a_M}\eta_S + \frac{b_M}{2\sqrt{a_M}}\right)},$$

$$a_M = \frac{\alpha_S}{\alpha_M'} \tag{45}$$

$$b_M = -2\left(1 - f_S\right)\eta_S \frac{\alpha_S}{\alpha_M}\left(\frac{\rho_S}{\rho_L} - 1\right)$$

$$\text{and } \frac{1}{\alpha_M'} = \frac{1}{\alpha_M} - \frac{\rho_M L_f}{k_M}\frac{\partial f_S}{\partial T_M} \tag{46}$$

The temperature distribution within solid, liquid and mushy zone is obtained from Eqs. (28), (29) and (44). These analytical expressions could be substituted in solidus and liquidus interface conditions (Eqs. 22 and 23) to obtain two nonlinear equations (Eqs. 47 and 48) which can be simultaneously solved to get the constants η_S and η_L.

$$\theta_E \frac{\exp\left(-\eta_S^2\right)}{erf\left(\eta_S\right)} - \frac{\sqrt{a_M}\, r_{MS}\theta_{liquidus} \exp\left(-\left(\sqrt{a_M}\eta_S + \frac{b_M}{2\sqrt{a_M}}\right)^2\right)}{erf\left(\sqrt{a_M}\eta_L + \frac{b_M}{2\sqrt{a_M}}\right) - erf\left(\sqrt{a_M}\eta_S + \frac{b_M}{2\sqrt{a_M}}\right)} = \frac{\sqrt{\pi}\eta_S\left(1 - f_{S,solidus}\right)}{St} \tag{47}$$

$$\frac{\sqrt{a_M}\, r_{MS}\theta_{liquidus} \exp\left(-\left(\sqrt{a_M}\eta_L + \frac{b_M}{2\sqrt{a_M}}\right)^2\right)}{erf\left(\sqrt{a_M}\eta_L + \frac{b_M}{2\sqrt{a_M}}\right) - erf\left(\sqrt{a_M}\eta_S + \frac{b_M}{2\sqrt{a_M}}\right)} + \frac{\sqrt{a_L}\, r_{LS}\theta_{initial} \exp\left(-\left(\sqrt{a_L}\eta_L + \frac{b_L}{2\sqrt{a_L}}\right)^2\right)}{erfc\left(\sqrt{a_L}\eta_L + \frac{b_L}{2\sqrt{a_L}}\right)} = \frac{\rho_L}{\rho_S}\frac{\sqrt{\pi} f_{S,liquidus}\eta_L}{St} \tag{48}$$

Where

$$a_M = \frac{\alpha_S}{\alpha_M'},\ b_M = -2\left(1 - f_S\right)\eta_S \frac{\alpha_S}{\alpha_M}\left(\frac{\rho_S}{\rho_L} - 1\right),$$

$$\frac{1}{\alpha_M'} = \frac{1}{\alpha_M} - \frac{\rho_M L_f}{k_M}\frac{\partial f_S}{\partial T_M}$$

$$a_L = \frac{\alpha_S}{\alpha_L} \text{ and } b_L = -2\eta_S \frac{\alpha_S}{\alpha_L}\left(\frac{\rho_S}{\rho_L} - 1\right)$$

For validation of expression obtained as given in Eqs. 47 and 48, the density variation term is switched off by substituting $R = 1$, which reduces the expressions for constant density as

$$\theta_E \frac{\exp\left(-\eta_S^2\right)}{erf\left(\eta_S\right)} - \frac{\sqrt{a_M}\, r_{MS}\theta_{liquidus} \exp\left(-\left(\sqrt{a_M}\eta_S\right)^2\right)}{erf\left(\sqrt{a_M}\eta_L\right) - erf\left(\sqrt{a_M}\eta_S\right)} = \frac{\sqrt{\pi}\eta_S\left(1 - f_{S,solidus}\right)}{St} \tag{49}$$

$$\frac{\sqrt{a_M}\, r_{MS}\theta_{liquidus}\exp\left(-\left(\sqrt{a_M}\eta_L\right)^2\right)}{erf\left(\sqrt{a_M}\eta_L\right)-erf\left(\sqrt{a_M}\eta_S\right)}+$$
$$+\frac{\sqrt{a_L}\, r_{LS}\theta_{initial}\exp\left(-\left(\sqrt{a_L}\eta_L\right)^2\right)}{erfc\left(\sqrt{a_L}\eta_L\right)}=$$
$$=\frac{\rho_L}{\rho_S}\frac{\sqrt{\pi}\, f_{S,liquidus}\eta_L}{St} \qquad (50)$$

Where

$$a_M=\frac{\alpha_S}{\alpha_M'},\ a_L=\frac{\alpha_S}{\alpha_L}\ \text{and}\ \frac{1}{\alpha_M'}=\frac{1}{\alpha_M}-\frac{\rho_M L_f}{k_M}\frac{\partial f_S}{\partial T_M}$$

4. Results and discussion

In the present analysis, a semi-analytical solution has been developed for solidification of a binary isomorphous alloy considering the effect of density change during phase transformation which may provide a benchmark for numerical testing of the numerical problems on binary alloy. Chakraborty and Dutta [15] proposed an exact solution for conduction dominated phase change solidification problem. The effect of microscopic models (lever rule model and scheil rule model) were investigated by analyzing the temperature and phase fraction distribution in all three phase regions (liquid, solid and mushy). However, the density was assumed to be constant which is a more simplistic assumption. In our previous work a similarity solution for one dimensional binary alloy solidification with shrinkage of expansion has been derived [17], while the interface was assumed to be sharp. Recently semi-analytical techniques have been proposed for binary alloy system [24,25] where the effect of shrinkage has been taken into account, but in our study we have derived it for pure analytical solution where the interface depth and movement of mushy zone is obtained tracking the liqudus interface and solidus interface individually.

As mentioned in section 2 (Problem description section), the thermo-physical properties like latent heat, thermal conductivity and specific heat in the mushy region are evaluated using the averaging technique, which varies with change in alloy composition during phase change. A systematic parametric study has been undertaken to study the effect of density variation (R) on interface motion and temperature distribution during phase transformation. Similarly, the effect of partition coefficient (k_p), initial temperature ($T_{initial}$) and boundary temperature (T_b) on solidification behavior is investigated in detail.

The temperature boundary conditions at $\eta = 0$ and $\eta \to \infty$ are taken respectively as $T_b = 1600$ K and $T_b = 1720$ K, while the initial temperature is taken as $T_{initial} = 1720$ *K* in the domain. The effect of density ratio on temperature distribution in the semi-infinite domain is shown in Fig. 3. It is found that density variation affects the liquidus interface motion. With increase in the density ratio (R) from 1 to 1.12, the liquidus interface moves faster. This is due to the larger quantity of heat removal by the alloy during solidification (due to increase in the density) which is more than compensated by shrinkage effect due to increase in the density. For more clarity, the solidus interface position (x_S) and the liquidus interface position (x_L) is plotted with time for different density ratio as shown in Fig. 4. It can be observed that the liquidus front (x_L) moves faster than the solidus front (x_S), making mushy zone to grow in size with passage of time. This is due to the fact that $\eta_L > \eta_S$, which makes liquidus front to move faster than solidus front. During later times, the difference between the position of liquidus fronts, while comparing two cases of density ratio ($R = 1$, $R = 1.12$) is quite visible.

TABLE 1

The thermo-physical material properties of pure Copper, pure Nickel and Cu-Ni binary alloy [Callister, 2007]

Element/Compound	Cu	Ni	0.05% Cu	0.1% Cu	0.15% Cu
Specific heat, C_p (J/Kg. K)	384	445	442	439	436
Thermal conductivity, k (W/m. K)	385	90	105	120	134
Latent heat of fusion, L_f (J/Kg)	131000	172000	169950	167900	165850
Density of solid phase, ρ_S Kg/m^3)	8908	8960	8957	8954	8952
Density of liquid phase, ρ_L Kg/m^3)	7810	8020	8000	7995	7989
		1.12	1.12	1.12	1.12
T_{melt} (K)	1630	1728	—	—	—
$T_{solidus}$ (K)	—	—	1693	1673	1653
$T_{liquidus}$ (K)	—	—	1713	1703	1693

The effect of species diffusion for both equilibrium and non-equilibrium solidification has been investigated thoroughly using Lever and Scheil's rule model as shown in Figs. 3-8. To study the comparison between these two model predictions, interface positions (solidus and liquidus) and temperature distribution have been plotted in the same figure (shown in Fig. 5) for different density ratios ($R = 1$, $R = 1.12$) and compositions (0.05%, 0.1% and 0.15%). On comparing these two microscopic transport models, some minor difference has been observed on the solidus and liquidus interface motion. While carefully looking at temperature distribution, deviation is noticed in temperature distribution predicted from both the models. This could be attributed behind the mechanism through which the solidification occurs using these two models. In Lever rule model, the species diffusion is assumed to be infinite in solid, while in case of Scheil's rule model, the species diffusion within solid phase is assumed to be absent. This is the plausible reason for this minor deviation in the result prediction by both these transport models.

To study the effect of composition change, an extensive study has been carried out, where interface positions (solidus and liquidus) and temperature distribution has been plotted for

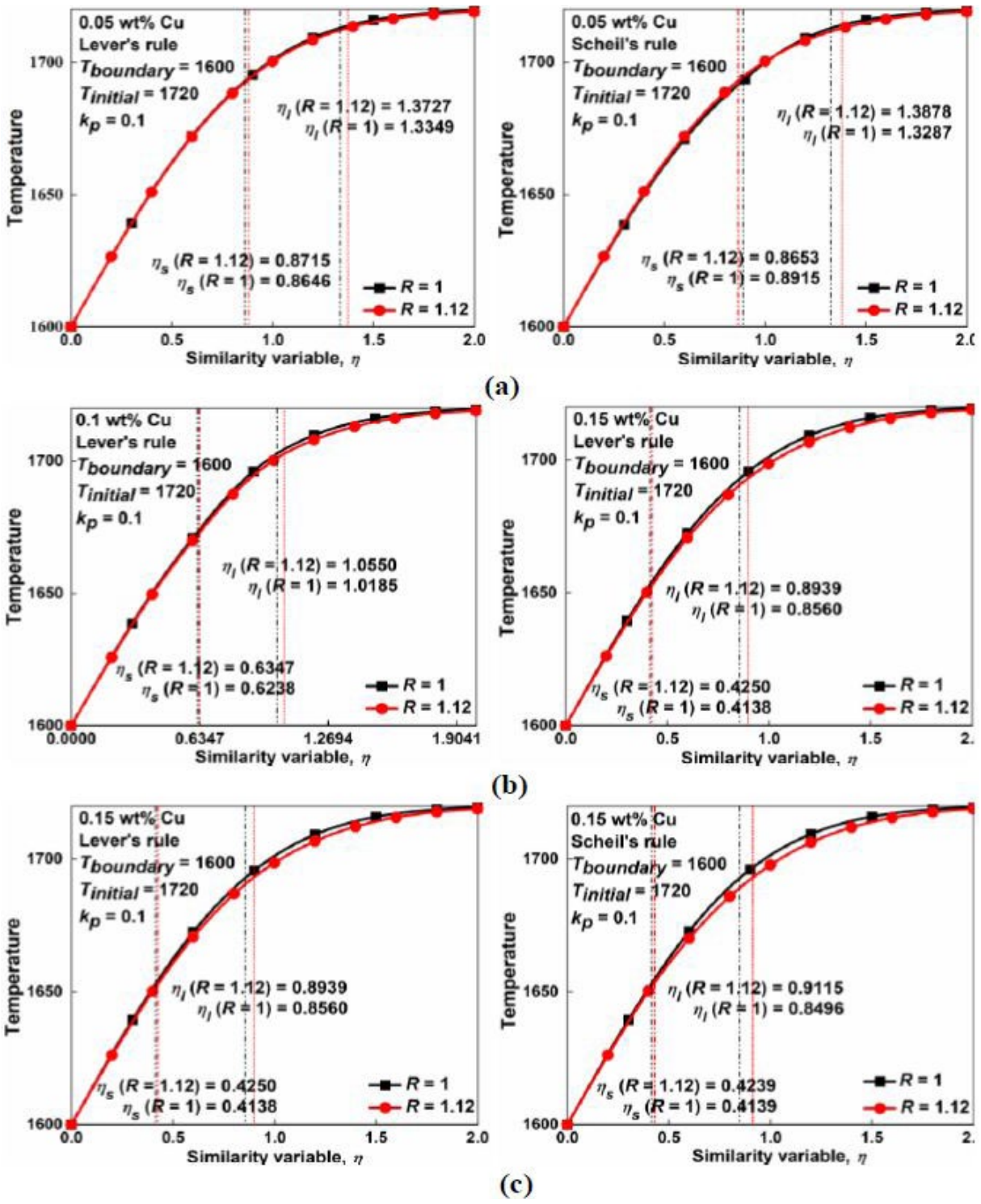

Fig. 3. Temperature distribution vs. similarity variable (η) in the semi-infinite domain for different initial composition ((a), (b) and (c)) of binary alloy as predicted from Lever rule model and Scheil's rule model for different density ratio (R = 1, R = 1.12)

three different compositions (0.05%, 0.1% and 0.15% Cu) as shown in Figs. 3-5. It can be observed that the interface moves slower with increase in the concentration of copper in the alloy. The liquidus temperature decreases with increase in the concentration of copper (as can be seen from the phase diagram shown in Fig. 2) due to which the onset of solidification gets delayed. As the liquidus temperature decreases, greater amount of sensible heat needs to be removed from the melt to reach to the particular phase change temperature (liquidus temperature), thus delaying the solidification process. The size of mushy zone is not much affected with change in composition. This could be attributed to the fact that heat removal rate from the boundary and latent heat of fusion (L_f) remains almost invariant with change in composition. The effect of initial and boundary temperature on solidification behavior of the binary alloy are shown in Figs. 6-7. Temperature distribution in the domain is

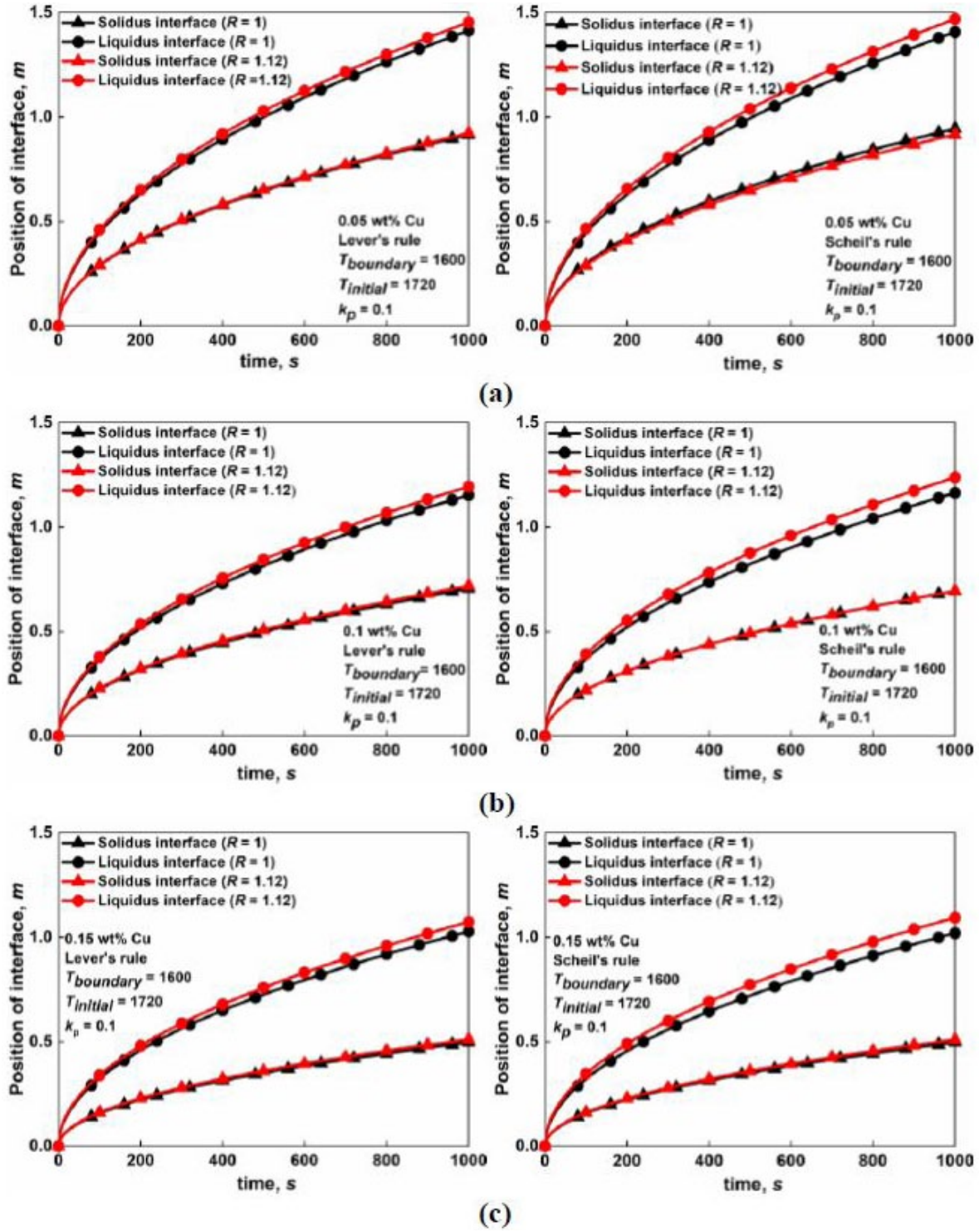

Fig. 4. Position of solidus interface (x_S) and liquidus interface (x_L) vs. time for different density ratio (R = 1, R = 1.12) and initial composition ((a), (b) and (c)) of binary alloy as predicted by lever and Scheil's rule

shown for three different boundary and initial temperatures. Results are compared for two different density ratios (R = 1, R = 1.12). Results predicted by two well-known solidification models: the lever rule model and Scheil's rule model are also shown side-by-side while studying the above effects. The effect of initial temperature of melt on solidification of the alloy is shown in Fig. 6. It is found that as the initial temperature increases, both solidus and liquidus fronts moves slower. This is because of the increase in the sensible heat content possessed by the material with increase in the initial temperature and hence a larger quantity of heat to be removed from the melt for the solidification to proceed. The size of the mushy zone is highly sensitive to change in initial temperature as can be seen from Fig. 6. It is found that with increase in initial temperature, the size of mushy zone decreases. This is due to the fact that as the initial temperature increases, the rate of heat removal in-

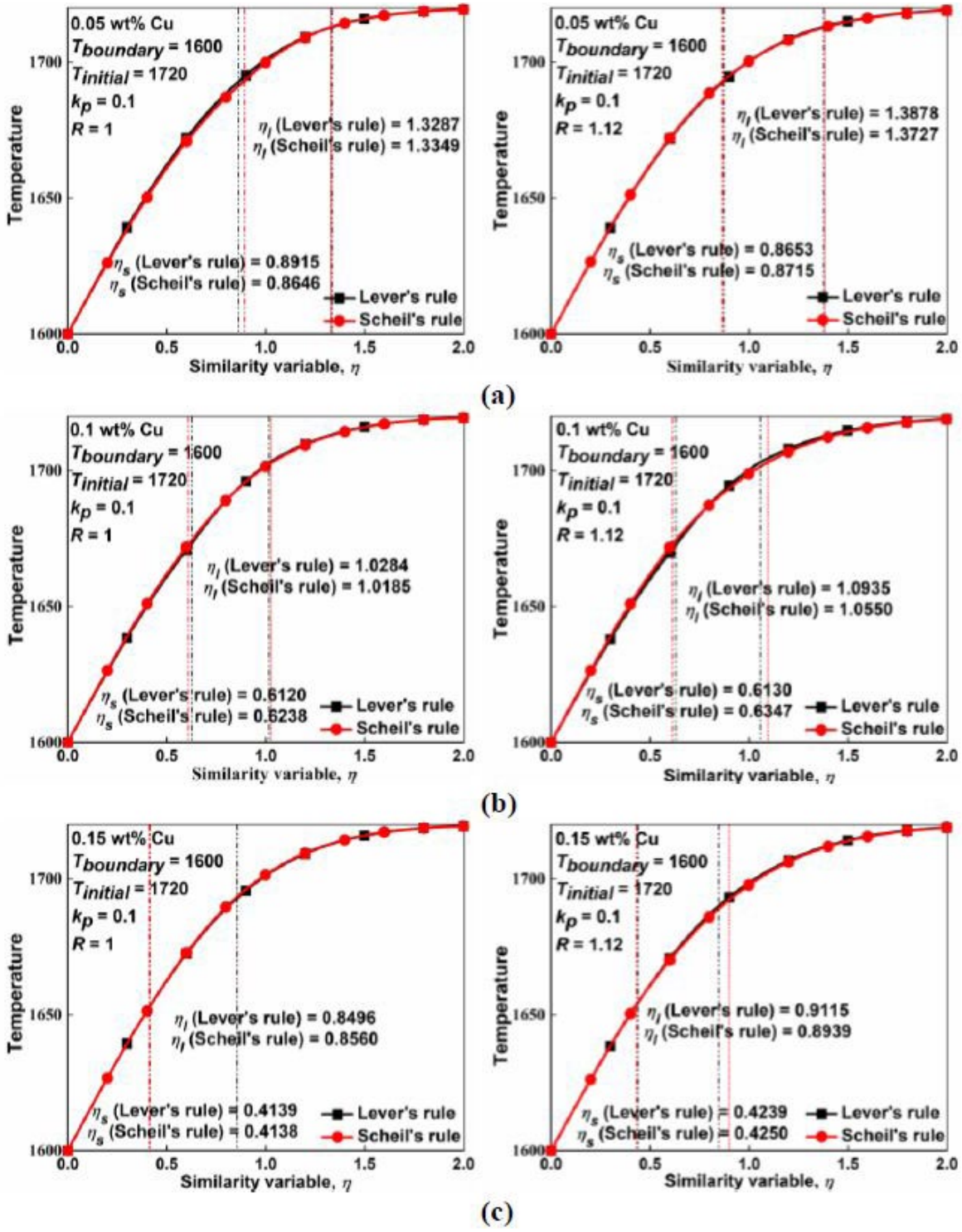

Fig. 5. Temperature distribution vs. similarity variable (η) in the semi-infinite domain for different density ratio (R = 1, R = 1.12) and initial concentration ((a), (b) and (c)) of binary alloy as predicted from Lever rule model and Scheil's rule model

creases, thereby decreasing the size of mushy zone. A similar solidification behavior is found while perturbing the boundary temperature as shown in Fig. 7. As the boundary temperature decreases, both the solidus and liquidus interface moves faster as predicted by both the solidification models.

One of the major reasons behind it is the increase in driving potential for heat removal at the boundary. As a result, both latent and sensible heat could be removed from the melt in shorter period of time resulting in faster movement of the interface. The partition coefficient plays a very important role in determining the distribution of solute within the solid and liquid phases respectively during phase transformation. During phase change the value of partition coefficient does not remain to be constant and is function of several parameters like nominal composition, solidification rate, mushy zone morphology, flow velocity of fluid within mushy zone, thermal and mass diffusivity etc.

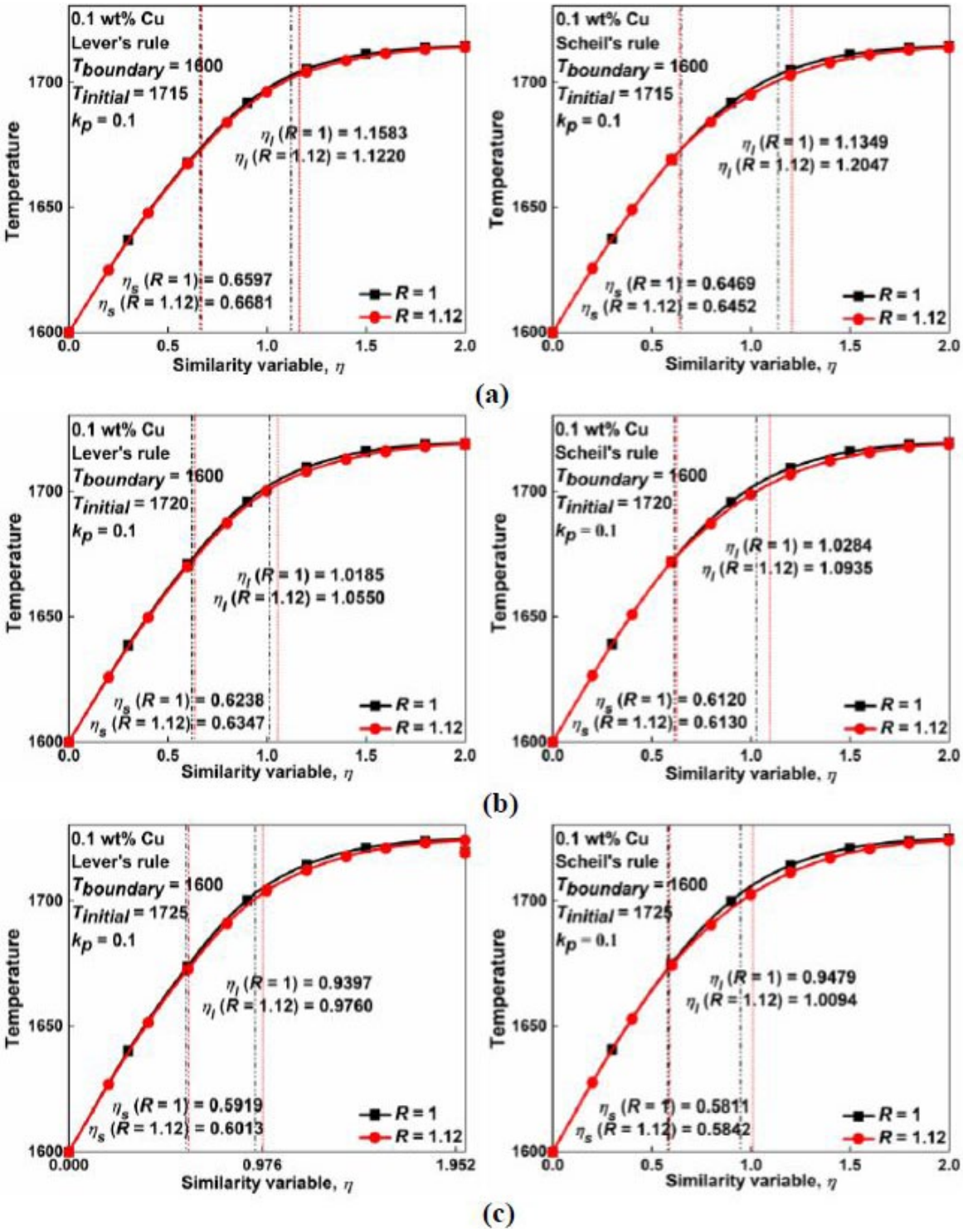

Fig. 6. Temperature distribution as a function of similarity variable (η) for different initial temperatures ($T_{initial}$) ((a), (b) and (c)) predicted from Lever rule model and Scheil's rule model for different density ratio (R = 1, R = 1.12)

However, in the present work the value of partition coefficient is assumed to be fixed for simplicity and ease of calculation based on the analytical approach. The effect of partition coefficient on the solidification behavior is shown in Fig. 8. The temperature distribution and interface positions plotted as a function of similarity variable (η) using both lever and Scheil's rule models for three different values of partition coefficient (k_p = 0.05, 0.1 and 0.2). The interface positions (solidus and liquidus) and temperature distribution is not much affected with increase in value of partition coefficient as can be seen from Fig. 8. This is because the latent heat of fusion remains invariant with change in partition coefficient values. Moreover, the rate of heat removal from the boundary remains constant with change in partition coefficient.

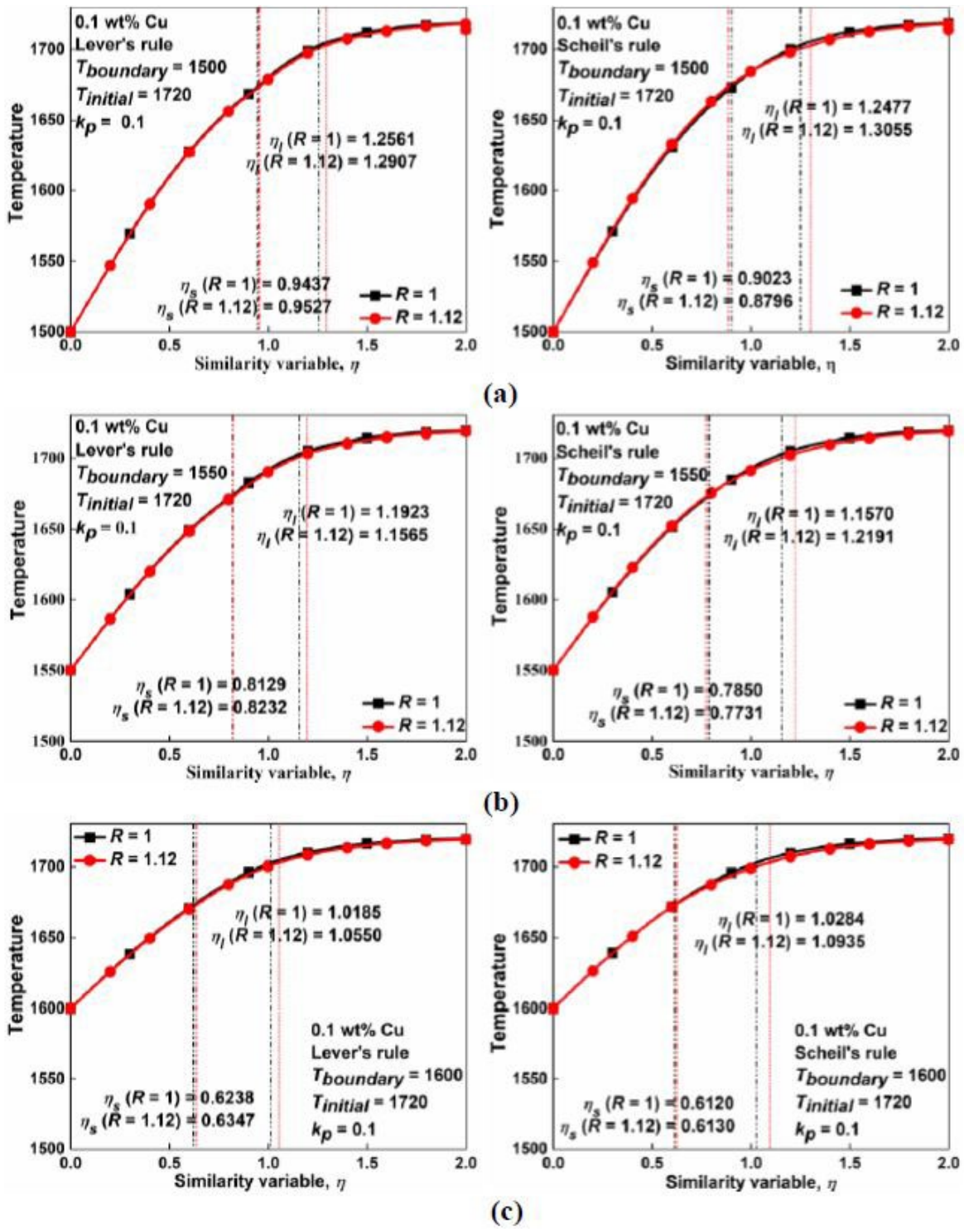

Fig. 7. Temperature distribution as a function of similarity variable (η) for different boundary temperatures (T_b) ((a), (b) and (c)) predicted from Lever rule model and Scheil's rule model for different density ratio (R = 1, R = 1.12)

5. Conclusions

A semi analytical solution has been developed for conduction dominated solidification of Cu-Ni binary alloy isomorphous system, where the density of liquid and solid is assumed to be different. Averaging technique was used to evaluate thermophysical properties and average phase fraction within the mushy zone. The effect of initial and boundary temperatures on the solidification behavior of the Cu-Ni binary isomorphous alloy have been also investigated in detail. The effect of equilibrium and non-equilibrium solidification was also analyzed using Lever and Scheil's rule models. Following few conclusions are made out of the detailed analysis. It can be concluded that density variation significantly affects the liquidus interface motion.

- Liquidus interface move faster with increase in the density ratio.

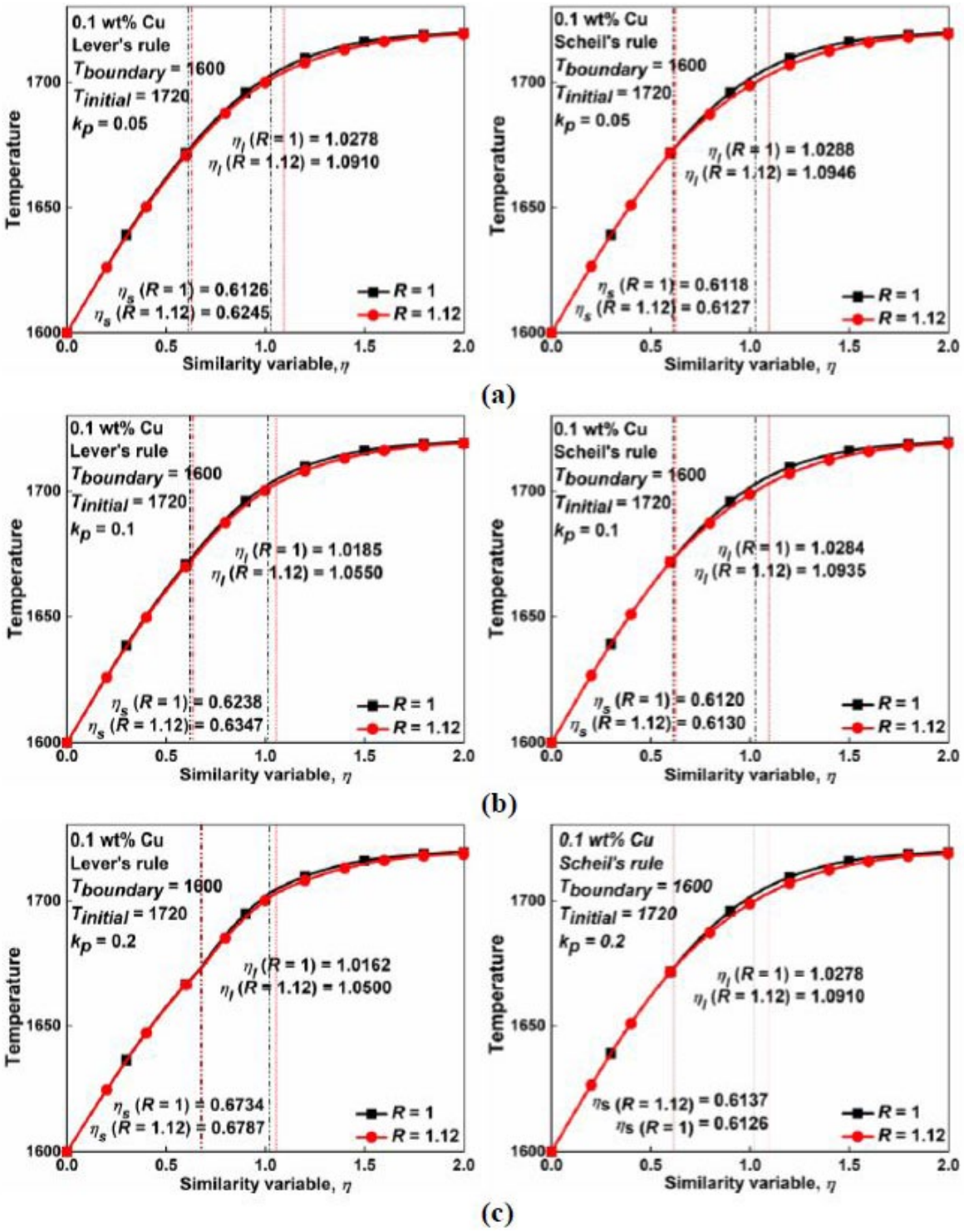

Fig. 8. Temperature distribution as a function of similarity variable (η) for different values partition coefficient (k_p) ((a), (b) and (c)) as predicted from Lever rule model and Scheil's rule model for different density ratio (R = 1, R = 1.12)

- It was found that both interfaces (solidus and liquidus) move faster with decrease in the initial temperature and boundary temperature.
- Minor deviation in the predicted temperature distribution and interface (solidus and liquidus) position was noticed in the solutions obtained from both the Lever and Scheil's rule models and change in partition coefficient values.

Acknowledgements

This work has been funded and supported by CSIR (Council of Scientific and Industrial Research) under the Shyama Prasad Mukherjee Fellowship Scheme with project number "SPM-06/1059(0210)/2014-EMR-I.

REFERENCES

[1] M.N. Ozisik, John Wiley & Sons **2**, 1-356 (1993).

[2] V. Alexiades, A.D. Solomon, Taylor & Francs **2**, 1-34 (1993).

[3] M. Turkyilmazoglu, Int. J. of Thermal. Sci. **126**, 67-73 (2018). DOI: https://doi.org/10.1016/j.ijthermalsci.2017.12.019

[4] A.N. Ceretani, D.A. Tarzia, Comput. and Appl. Math. **37** (2), 2201-2217 (2018). DOI: https://doi.org/10.1007/s40314-017-0442-0

[5] L. Barannyk, S.D. Williams, O.I. Ogidan, J.C. Crepeau, A. Sakhnov, Heat Transfer Summer Conference, ASME **59315**, V001T10A014, (2019). DOI: https://doi.org/10.1115/HT2019-3703

[6] M. Parhizi, A. Jain, J. of Heat Trans. **141** (2), (2019). DOI: https://doi.org/10.1115/1.4041956

[77] S.L. Tariq, H.M. Ali, M.A. Akram, M.M. Janjua, M. Ahmadlouydarab, Appl. Therm. Engg. **176**, 115305, (2020). DOI: https://doi.org/10.1016/j.applthermaleng.2020.115305

[8] A. Agarwal, R.M Sarviya, Engg. Sci. and Tech., An Int. J. **19** (1), 619-631 (2016). DOI: https://doi.org/10.1016/j.jestch.2015.09.014

[9] S. Chakraborty, P. Dutta, Metall. and Mat. Trans. **32** (3), 562 (2001). DOI: https://doi.org/10.1007/s11663-001-0042-6

[10] E.S. Jafar, M. Eslamian, M.Z. Saghir, Engg. Sci. and Tech., and Int. J. **19** (1), 511-517 (2016).

[11] V.R. Voller, A.D. Brent, C. Prakash, Int. J. of Heat and Mass Trans. **32** (9), 1719-1731 (1989).

[12] V.R. Voller, A.D. Brent, C. Prakash, Appl. Math. Modell. **14** (6), 320-326 (1990).

[13] V.R. Voller, Int. J. of Heat and Mass Trans. **51** (3), 823-834 (2008).

[14] J.D. Chung, J.S. Lee, S.T. Ro, H. Yoo, Int. J. of Heat and Mass Trans. **42** (2), 373-377 (1999).

[15] S. Chakraborty, P. Dutta, Appl. Math. Modell. **26** (4), 545-561 (2002).

[16] V.R. Voller, Int. J. of Heat and Mass Trans. **49** (11), 1981-19 (2006).

[17] A. Jakhar, A. Bhattacharya, P. Rath, S.K. Mahapatra, Int. J. of Heat and Mass Trans. **127**, 1114-1127 (2018).

[18] M. Assuncao, M. Vynnycky, S.L Mitchel, Eur. J. Appl. Math. (2020). DOI: https://doi.org/10.1017/ S0956792520000091

[19] F.B. Planella, C.P. Please, R.A. Van Gorder, J. of Appl. Math. **83** (1), 106-130 (2018).

[20] F.B. Planella, C.P. Please, R.A. Van Gorder, J. of Appl. Math. **79** (3), 876-913 (2019).

[21] F.B. Planella, C.P. Please, R.A. Van Gorder, Eur. J. Appl. Math. **32** (2), 242-279 (2021).

[22] V. Chaurasiya, D. Kumar, K.N. Rai, J.A. Singh Therm. Sci. Engg. Proc. **20**, 100664 (2020).

[23] P. Levi, N. Ascherson, Schocken Books, New York, **2**, 1-30, (1984).

[24] M. Vynnycky, S. Saleem, H. Fredriksson, Appl. Math. Mod. **54**, 605-626 (2018).

APPENDIX A

Derivation of Similarity Transformation for Solid, Liquid and Mushy Zone Phase

Using the similarity transformation parameter $\eta = xg(t)$, where $g(t) = 1/2\sqrt{\alpha_S t}$. Implementing similarity transformation, in Eqs. 16, 17 and 18, we get a set of transformed equations for solid, liquid and mushy phase whose derivation has been given in detail below.

Solid phase

$$\frac{\partial \theta_S}{\partial t} = \frac{\partial \theta_S}{\partial \eta}\frac{\partial \eta}{\partial t} = x\frac{\partial g}{\partial t}\frac{\partial \theta_S}{\partial \eta} \tag{A.1}$$

$$\frac{\partial^2 \theta_S}{\partial x^2} = \frac{\partial^2 \theta_S}{\partial \eta^2}\left(\frac{\partial \eta}{\partial x}\right)^2 = g^2\frac{\partial^2 \theta_S}{\partial \eta^2} \tag{A.2}$$

$$\frac{1}{\alpha_S}x\frac{\partial g}{\partial t}\frac{\partial \theta_S}{\partial \eta} = g^2\frac{\partial^2 \theta_S}{\partial \eta^2} \tag{A.3}$$

On substituting $x = \eta/g(t)$ in the above equation we would get

$$\frac{\partial^2 \theta_S}{\partial \eta^2} = \frac{\eta}{\alpha_S}\frac{dg/dt}{g^3}\frac{\partial \theta_S}{\partial \eta} \tag{A.4}$$

Where, $g(t) = \dfrac{1}{2\sqrt{\alpha_S t}}$ which could be written as $\dfrac{\partial g}{\partial t} = \dfrac{-1}{4t\sqrt{\alpha_S t}}$.

On substituting expression A.1, A.2, A.3 and A.4 in Equation 16, we would get

$$\frac{\partial^2 \theta_S}{\partial \eta^2} + 2\eta\frac{\partial \theta_S}{\partial \eta} = 0 \text{ for } 0 < \eta < \eta_S \tag{A.5}$$

Mushy zone phase

$$\frac{\partial \theta_M}{\partial t} = \frac{\partial \theta_M}{\partial \eta}\frac{\partial \eta}{\partial t} = x\frac{\partial g}{\partial t}\frac{\partial \theta_M}{\partial \eta} \tag{A.6}$$

$$\frac{\partial \theta_M}{\partial x} = \frac{\partial \theta_M}{\partial \eta}\frac{\partial \eta}{\partial x} = g\frac{\partial \theta_M}{\partial \eta} \tag{A.7}$$

$$\frac{\partial^2 \theta_M}{\partial x^2} = \frac{\partial^2 \theta_M}{\partial \eta^2}\left(\frac{\partial \eta}{\partial x}\right)^2 = g^2\frac{\partial^2 \theta_M}{\partial \eta^2} \tag{A.8}$$

Similarly substituting A.6, A.7 and A.8 in Eq. (17) we would get expression A.9.

$$\left(\frac{1}{\alpha_M}-\frac{\rho L_f}{k_M}\frac{\partial f_S}{\partial T_M}\right)x\frac{\partial g}{\partial t}\frac{\partial \theta_M}{\partial \eta}+$$
$$+\frac{(1-f_S)}{\alpha_M}\left(\frac{\rho_S}{\rho_L}-1\right)\frac{dx_S}{dt}g\frac{\partial \theta_M}{\partial n}=g^2\frac{\partial^2\theta_M}{\partial \eta^2} \quad (A.9)$$

The position of solidus front would be given by $x_S=2\eta_S\sqrt{\alpha_S t}$ and $\frac{dx_S}{dt}=\frac{\eta_S\sqrt{\alpha_S}}{\sqrt{t}}$.

Substituting the above expression in A.9 we get

$$\left(\frac{1}{\alpha_M}-\frac{\rho L_f}{k_M}\frac{\partial f_S}{\partial T_M}\right)\frac{-x}{4t\sqrt{\alpha_S t}}\frac{\partial \theta_M}{\partial \eta}+$$
$$+\frac{(1-f_S)}{\alpha_M}\left(\frac{\rho_S}{\rho_L}-1\right)\frac{\eta_S\sqrt{\alpha_S}}{\sqrt{t}}\frac{1}{2\sqrt{\alpha_S t}}\frac{\partial \theta_M}{\partial n}=$$
$$=\frac{1}{4\alpha_S t}\frac{\partial^2\theta_M}{\partial \eta^2} \quad (A.10)$$

On rearranging we would get,

$$-\left(\frac{1}{\alpha_M}-\frac{\rho L_f}{k_M}\frac{\partial f_S}{\partial T_M}\right)2\eta\frac{\partial \theta_M}{\partial \eta}+$$
$$+\frac{(1-f_S)}{\alpha_M}\left(\frac{\rho_S}{\rho_L}-1\right)2\eta_S\frac{\partial \theta_M}{\partial n}=\frac{1}{\alpha_S}\frac{\partial^2\theta_M}{\partial \eta^2} \quad (A.11)$$

Substituting $\frac{1}{\alpha'_M}=\frac{1}{\alpha_M}-\frac{\rho L_f}{k_M}\frac{\partial f_S}{\partial T_M}$

$$\frac{\partial^2\theta_M}{\partial \eta^2}+\left(2\frac{\alpha_S}{\alpha'_M}\eta-2(1-f_S)\eta_S\frac{\alpha_S}{\alpha_M}\left(\frac{\rho_S}{\rho_L}-1\right)\right)\frac{\partial \theta_M}{\partial \eta}=0 \quad (A.12)$$

This could be written in form

$$\frac{\partial^2\theta_M}{\partial \eta^2}+(2a_M\eta+b_M)\frac{\partial \theta_M}{\partial \eta}=0 \text{ for } \eta_L<\eta<\eta_S \quad (A.13)$$

Where

$$a_M=\frac{\alpha_S}{\alpha'_M},\ b_M=-2(1-f_S)\eta_S\frac{\alpha_S}{\alpha_M}\left(\frac{\rho_S}{\rho_L}-1\right)$$

and $\frac{1}{\alpha'_M}=\frac{1}{\alpha_M}-\frac{\rho L_f}{k_M}\frac{\partial f_S}{\partial T_M}$

Liquid phase

$$\frac{\partial \theta_L}{\partial t}=\frac{\partial \theta_L}{\partial \eta}\frac{\partial \eta}{\partial t}=x\frac{\partial g}{\partial t}\frac{\partial \theta_L}{\partial \eta} \quad (A.14)$$

$$\frac{\partial \theta_L}{\partial t}=\frac{\partial \theta_L}{\partial \eta}\frac{\partial \eta}{\partial x}=g\frac{\partial \theta_L}{\partial \eta} \quad (A.15)$$

$$\frac{\partial^2\theta_L}{\partial x^2}=\frac{\partial^2\theta_L}{\partial \eta^2}\left(\frac{\partial \eta}{\partial \eta}\right)^2=g^2\frac{\partial^2\theta_L}{\partial \eta^2} \quad (A.16)$$

Using expression A.14, A.15 and A.16 and substituting it in Eq. 18 we would get expression, given by A.17.

$$\frac{1}{\alpha_L}x\frac{\partial g}{\partial t}\frac{\partial \theta_L}{\partial \eta}+\frac{1}{\alpha_L}\left(\frac{\rho_S}{\rho_L}-1\right)\frac{dx_S}{dt}g\frac{\partial \theta_L}{\partial \eta}=$$
$$=g^2\frac{\partial^2\theta_L}{\partial \eta^2},\ \eta_L<\eta<\infty \quad (A.17)$$

The position of solidus front would be given by $x_S=2\eta_S\sqrt{\alpha_S t}$ and $\frac{dx_S}{dt}=\frac{\eta_S\sqrt{\alpha_S}}{\sqrt{t}}$

On substituting it in expression A.17 we would get,

$$\frac{1}{\alpha_L}\frac{-x}{4t\sqrt{\alpha_S t}}\frac{\partial \theta_L}{\partial \eta}+\frac{1}{\alpha_L}\left(\frac{\rho_S}{\rho_L}-1\right)\frac{\eta_S\sqrt{\alpha_S}}{\sqrt{t}}\frac{1}{2\sqrt{\alpha_S t}}\frac{\partial \theta_L}{\partial \eta}=$$
$$=\frac{1}{4\alpha_S t}\frac{\partial^2\theta_L}{\partial \eta^2},\ \eta_L<\eta<\infty \quad (A.18)$$

On rearranging the given expression A.18.

$$\frac{\partial^2\theta_L}{\partial \eta^2}+\left(2\frac{\alpha_S}{\alpha_L}\eta-2\eta_S\frac{\alpha_S}{\alpha_L}\left(\frac{\rho_S}{\rho_L}-1\right)\right)\frac{\partial \theta_L}{\partial \eta}=0 \quad (A.19)$$

Which could be written as

$$\frac{\partial^2\theta_L}{\partial \eta^2}+(2\alpha_L\eta+b_L)\frac{\partial \theta_L}{\partial \eta}=0 \text{ for } \eta_L<\eta<\infty \quad (A.20)$$

Where

$$\alpha_L=\frac{\alpha_S}{\alpha_L} \text{ and } b_L=-2\eta_S\frac{\alpha_S}{\alpha_L}\left(\frac{\rho_S}{\rho_L}-1\right)$$

APPENDIX B

$$\frac{\partial^2 \theta_M}{\partial \eta^2} + \left(2\alpha_M \eta + b_M\right)\frac{\partial \theta_M}{\partial \eta} = 0 \tag{B.1}$$

The above equation could be re-written as

$$\frac{\partial^2 \theta_M}{\partial \eta^2} + 2\sqrt{\alpha_M}\left(\sqrt{\alpha_M}\,\eta + \frac{b_M}{2\sqrt{a_M}}\right)\frac{\partial \theta_M}{\partial \eta} = 0 \tag{B.2}$$

Putting

$$t = \sqrt{\alpha_M}\,\eta + \frac{b_M}{2\sqrt{a_M}} \tag{B.3}$$

$$\frac{\partial^2 \theta_M}{\partial \eta^2} = \frac{\partial^2 \theta_M}{\partial t^2}\left(\frac{\partial t}{\partial \eta}\right)^2 = \alpha_M \frac{\partial^2 \theta_M}{\partial t^2} \tag{B.4}$$

$$\frac{\partial \theta_M}{\partial \eta^2} = \frac{\partial \theta_M}{\partial t}\frac{\partial t}{\partial \eta} = \sqrt{\alpha_M}\frac{\partial \theta_M}{\partial t^2} \tag{B.5}$$

Using expressions in the Eqs. B.2, B.3, B.4 and B.5.

$$a_M \frac{\partial^2 \theta_M}{\partial \eta^2} + 2a_M t \frac{\partial \theta_M}{\partial t} = 0 \tag{B.6}$$

Which could be written as,

$$\frac{\partial^2 \theta_M}{\partial \eta^2} + 2t\frac{\partial \theta_M}{\partial t} = 0 \text{ where } t = \sqrt{a_M}\,\eta + \frac{b_M}{2\sqrt{a_M}} \tag{B.7}$$

Eq. B.7, is and ODE which could be written as

$$\frac{\partial^2 \theta_M}{\partial \eta^2} + 2t\frac{\partial \theta_M}{\partial t} = 0 \tag{B.8}$$